Revisiting Oceanic Acoustic Gravity Surface Waves

JEROME A. SMITH

Scripps Institution of Oceanography, University of California, San Diego, La Jolla, California

(Manuscript received 18 December 2014, in final form 11 September 2015)

ABSTRACT

The reintroduction of compressibility into the equations for surface gravity waves can permit mixed acoustic–gravity modes that are periodic in the vertical as well as horizontal directions. These modes interact with the bottom even in deep water, so bottom motion can excite them. Because they propagate rapidly, it has been suggested they may be useful as precursors of tsunamis. Here the equations are revisited, and, using some robust approximations, some physical understanding and interpretation of the phenomena are presented. It is posed that these new modes can alternatively be thought of as acoustic modes slightly modified by a gravity wave boundary condition at the surface, rather than as surface waves dramatically modified by compressibility. Their potential use is not diminished; indeed, this alternative perspective should help make implementation more practical.

1. Introduction

Although first described over 100 years ago (e.g., Pidduck 1912), there has been a recent rekindling of interest in oceanic acoustic–gravity surface waves, in particular in the context of tsunamis (e.g., Stiassnie 2010; Kadri and Stiassnie 2012; Hendin and Stiassnie 2013; Abdolali et al. 2015; Cecioni et al. 2015). It has also been suggested that they can contribute to deep water transport (Kadri 2014).

The original derivation is a bit hard to follow, so in the spirit of independent verification, and to bring a different perspective, it seems worthwhile to rederive the basic results. The emphasis here is on simplicity and clarity, as well as outlining the assumptions made. In addition, some typical oceanic values (e.g., speed of sound $\sim$1500 m s^{-1}, ocean depth $\sim$4000 m) are used to identify insignificant terms via scale analysis and reveal the most important dynamics. The intent of this work is to provide a brief review and a simplified introduction to the phenomenon, with a brief list of references for more complete and rigorous treatments; for a more rigorous treatment, the reader is referred to Watada (2013), or to introductory text books on acoustics such as Jensen et al. (2011) or Tolstoy and Clay (1987). To help define terminology and provide a clear foundation, the analysis here starts with very basic relations and progresses to increasing specificity.

With finite compressibility, the condition of nondivergence is replaced by mass continuity:

$$\partial_t \rho + (\mathbf{u} \cdot \nabla)\rho = -\rho \nabla \cdot \mathbf{u}, \tag{1.1}$$

where ∂_t denotes the time derivative, ρ is the density, $\mathbf{u}$ is the velocity vector, $(\mathbf{u} \cdot \nabla)$ denotes the advective part of the material derivative, and $\nabla \cdot \mathbf{u}$ is the divergence (e.g., Lamb 1932, p. 5). For adiabatic compression, the change in pressure p corresponding to a change in density is

$$\partial_\rho p = C_S^2, \tag{1.2}$$

where C_S is the speed of sound in the water (e.g., Lamb 1932, p. 477), taken as 1500 m s^{-1} for the examples considered below. This relation holds in a Lagrangian frame of reference, that is, moving with the fluid; thus, the material rate of change in pressure is related to that of density via (1.2) and the chain rule, and then to the divergence via (1.1):

$$\partial_t p + (\mathbf{u} \cdot \nabla)p = C_S^2[\partial_t \rho + (\mathbf{u} \cdot \nabla)\rho] = -\rho C_S^2 \nabla \cdot \mathbf{u}. \tag{1.3}$$

For simplicity, consider 2D waves (x and z) and uniform density other than fluctuations caused by compression in response to pressure. It is useful to define the background

Denotes Open Access content.

Corresponding author address: Jerome A. Smith, Scripps Institution of Oceanography, University of California, San Diego, 8851 Shellback Way, La Jolla, CA 92093.
E-mail: jasmith@ucsd.edu

DOI: 10.1175/JPO-D-14-0256.1

© 2015 American Meteorological Society

pressure and density, p_b and ρ_b, respectively, that would exist without the wavelike fluctuations (which are assumed small). With gravity parallel to z, these vary only with depth, so, to first order in the fluctuations (denoted by primes), (1.3) becomes

$$\partial_t p' + w'\partial_z p_b = C_S^2(\partial_t \rho' + w'\partial_z \rho_b) = -\rho C_S^2 \nabla \cdot \mathbf{u}'. \quad (1.4)$$

For background pressure and density fields in compressional equilibrium, $\partial_z p_b = C_S^2 \partial_z \rho_b$, so the first equality in (1.4) implies that $p' = C_S^2 \rho'$ (for zero-mean fluctuations the constant of integration in time is set to zero). This equilibrium relation also implies that $\rho_b = \rho_0 + C_S^{-2} p_b$, where ρ_0 is constant in z. Then the background pressure is found by solving

$$p_b = -g\int_0^z \rho_b \, dz = -g\left(\rho_0 z + C_S^{-2}\int_0^z p_b \, dz\right) \quad (1.5a)$$

or, taking the z derivative,

$$\partial_z p_b + gC_S^{-2} p_b + g\rho_0 = 0. \quad (1.5b)$$

This has the solution

$$p_b = Be^{-(g/C_S^2)z} - \rho_0 C_S^2 = \rho_0 C_S^2[e^{-(g/C_S^2)z} - 1], \quad (1.6)$$

where the constant B was chosen so that $p_b = 0$ at $z = 0$. If atmospheric pressure is applied at the surface, it adds to the exponential term; alternatively, an offset (e.g., about 10 m) could be added to z in the exponent. Expanding the exponential as a series, the first term is the "usual" hydrostatic pressure, $-g\rho_0 z$; then, even at 4000 m depth, the next term is smaller by a factor of over 110. It is worth noting that, while ρ_0 dominates in the ocean, it would be zero in an ideal gas, or (roughly) in the atmosphere, and the pressure would be just an exponential with a constant factor determined by the surface pressure (i.e., the total weight of the atmosphere). Indeed, it is worth noting that few of the simplifying approximations made here would be justified in the atmosphere.

Ignoring rotation and dissipation, and removing the background balance $\nabla p_b + \rho_b g = 0$, the momentum equation can be written to first order in the fluctuations as

$$\rho_0 \partial_t \mathbf{u}' + \nabla p' + \rho' g = \rho_0 \partial_t \mathbf{u}' + \nabla p' + (gC_S^{-2})p' = 0. \quad (1.7)$$

The ratio of magnitudes of the last term to the middle one on the left-hand side is $g\lambda/2\pi C_S^2$, where λ is the wavelength of the perturbation; so the last term is negligible if $\lambda \ll 2\pi C_S^2/g \approx 1414$ km. The longest waves to be considered here are about 4 times the ocean depth, say $\lambda < 16$ km, so this last term is smaller by a factor of at least 87 and can be discarded.

Since the flow is irrotational, both the pressure and velocity can be cast in terms of a velocity potential φ such that $\mathbf{u} = \nabla\varphi$. In terms of this, (1.7) becomes (dropping the primes and the negligible term involving gravity):

$$\partial_t \mathbf{u} = \partial_t \nabla\varphi = \nabla\partial_t\varphi = -\rho_0^{-1}\nabla p, \quad (1.8)$$

so we identify the pressure as $p = -\rho_0 \partial_t \varphi$ (both having zero mean). Returning to the continuity equation (1.4), we have

$$-\rho_0^{-1}\partial_t p = C_S^2 \nabla \cdot \mathbf{u} - wg \quad \text{or} \quad \partial_t^2 \varphi = C_S^2 \nabla^2 \varphi - g\partial_z \varphi. \quad (1.9)$$

The ratio of magnitudes of the last term to the other on the right-hand side is no larger than $g\lambda/2\pi C_S^2$ (again), so the last term here is also negligible. Thus, to a good approximation, gravity has little effect on the perturbations in the fluid interior; it enters primarily via the surface boundary condition (discussed below).

For horizontally propagating waves in general, we seek solutions of the form

$$\varphi = Na\cos(mx - \omega t)f(z), \quad (1.10)$$

where N is a normalization constant, a is the amplitude, m is the horizontal wavenumber, ω is the radian frequency, and $f(z)$ is a vertical function that satisfies the surface and bottom boundary conditions. Defining ζ as the surface displacement, we require the perturbations to obey: at $z = 0$,

$$p \equiv -\rho_0 \partial_t \varphi = \rho_0 g\zeta \equiv \rho_0 g\int^t \partial_z \varphi \, dt,$$

or, taking a time derivative,

$$\rho_0^{-1}\partial_t p \equiv -\partial_t^2 \varphi = \omega^2 \varphi = g\partial_z \varphi. \quad (1.11)$$

Meanwhile, at $z = -h$, a rigid-bottom boundary condition is applied [this is probably all right for a hard-rock bottom, but see the discussion after (3.5) below]:

$$w = \partial_z \varphi = 0. \quad (1.12)$$

An obvious (and standard) choice for f is $f(z) = \cosh[n(z + h)]$, where n is a vertical wavenumber (not necessarily equal to m). This satisfies (1.12) immediately; the surface boundary condition [(1.11)] then implies the familiar-looking surface wave linear dispersion relation (note this involves the vertical wavenumber n, and not m):

$$\omega^2 = gn\tanh(nh). \quad (1.13)$$

Putting this solution for φ into the modified (slightly compressible) equation for continuity [(1.9), dropping the last term as noted] yields a wavenumber equation:

$$m^2 - n^2 = C_S^{-2}\omega^2 \quad \text{or} \quad m^2 = n^2 + C_S^{-2}\omega^2 . \tag{1.14}$$

To accommodate slight compressibility with real vertical wavenumber n, the horizontal wavenumber is slightly larger than the vertical. For typical surface wave frequencies, and for real n, this correction is very small and decreases with decreasing frequency. Indeed, for this term to become significant would require frequencies well into the capillary wave regime, for which the above analysis is not valid.

2. The "new" modes

The interesting thing about the modified (compressible) wavenumber equation [(1.14)] is that it permits solutions with both real m and imaginary n in addition to the usual surface wave solution at a given frequency. These "new" solutions are oscillatory in both x and z: they do not fade out with depth. Also, there can be a whole set of such solutions, not just one. Substituting $in_j = n$ in the above for the jth solution, the vertical function transforms into

$$f_j(z) = \cosh[in_j(z+h)] = \cos[n_j(z+h)], \tag{2.1}$$

which still satisfies the bottom boundary condition [(1.12)]. Here, the subscript $j = 1$ will denote the smallest (gravest) such mode, and we retroactively assign the subscript 0 to the "usual" surface wave mode of section 1. The surface boundary condition [(1.11)] becomes

$$\omega^2 = -gn_j \tan(n_j h). \tag{2.2}$$

Remarkably, (2.2) is also just what is required for f_j to be orthogonal to f_0:

$$\begin{aligned} 0 &= \int_{-h}^{0} f_0 f_j \, dz = \int_0^h \cosh(n_0 z)\cosh(in_j z)\, dz \\ &= 0.5\int_0^h \{\cosh[(n_0 + in_j)z] + \cosh[(n_0 - in_j)z]\}\, dz \\ &= (\text{const})[n_0 \sinh(n_0 h)\cos(n_j h) + n_j \cosh(n_0 h)\sin(n_j h)]. \end{aligned} \tag{2.3}$$

Multiplying all by $g/[\cos(n_j h)\cosh(n_0 h)]$, this last expression equaling 0 is found to mean

$$gn_0 \tanh(n_0 h) = -gn_j \tan(n_j h) = \omega^2, \tag{2.4}$$

just as in (2.2).

For the right-hand side in (2.2) [or (2.4)] to be positive, n_j and $\tan(n_j h)$ must have opposite signs. The smallest (gravest) solution for $n_1 h$ ($j = 1$) must therefore lie between $\pi/2$ and π. To gain insight, let's explore the behavior just past $\pi/2$: let $n_1 h = \pi/2 + b$, where b is small. Then

$$\begin{aligned} \tan(n_1 h) &= \tan(\pi/2 + b) = -\cot(b) \approx -1/b \\ &= -1/(n_1 h - \pi/2), \end{aligned} \tag{2.5}$$

and so

$$\omega^2 = -gn_1 \tan(n_1 h) \approx \frac{gn_1}{n_1 h - \pi/2} \tag{2.6}$$

or

$$n_1 \approx \frac{\pi}{2}\left(\frac{\omega^2}{h\omega^2 - g}\right) = \frac{\pi}{2}\left(\frac{k_d}{k_d h - 1}\right), \tag{2.7}$$

where $k_d \equiv \omega^2/g$ is the familiar deep water wavenumber solution at frequency ω (see also Kadri 2015, appendix A). For validity, we require $k_d h > 1$, that is, $\omega^2 > g/h$. For example, if $h = 4000$ m, then $\omega > 0.05$ rad s^{-1}, implying a wave period $T < 126$ s. In fact, to simplify this further, let us assume $k_d h \gg 1$, so (2.7) reduces to

$$n_1 \approx \frac{\pi}{2h}\left(\frac{1}{1 - 1/k_d h}\right) \approx \frac{\pi}{2h}\left(1 + \frac{1}{k_d h}\right) = \frac{\pi}{2h}\left(1 + \frac{g}{h\omega^2}\right). \tag{2.8}$$

To the same level of approximation,

$$n_1^2 \approx \left(\frac{\pi}{2h}\right)^2\left(1 + \frac{2g}{h\omega^2}\right) = \left(\frac{\pi}{2h}\right)^2 + \frac{g\pi^2}{2h^3\omega^2}, \tag{2.9}$$

and so

$$m_1^2 = \frac{\omega^2}{C_S^2} - n_1^2 \approx \frac{\omega^2}{C_S^2} - \left(\frac{\pi}{2h}\right)^2 - \frac{g\pi^2}{2h^3\omega^2}. \tag{2.10}$$

Ignoring the last term for now, it is already clear that for m_1 to be real,

$$\omega \geq \omega_{\min} > \pi C_S/2h. \tag{2.11}$$

With $C_S = 1500$ m s^{-1} and $h = 4000$ m, $\omega_{\min} > 0.589$ rad s^{-1}, corresponding to a maximum wave period of about 10.67 s. At that frequency, the last term in 2.10 would be about -2.2×10^{-9}, whereas the first terms are each about 1.54×10^{-7}, some 71 times larger. Including the last term results in a quadratic equation for $\omega_{\min}^2$ and raises the solution to about 0.593 rad s^{-1}, which is less than a 1% correction, and is probably within the error

bounds of other terms neglected (e.g., nonlinearity, sound-speed variations). At higher frequencies it is even less significant. Also, since $\omega_{\min}$ is approximately proportional to $1/h$, the neglected term decreases in importance relative to the first two terms in shallower water as well.

Next, consider the horizontal group velocity $\partial_{m_1}\omega$. We start "upside down" with

$$\partial_\omega m_1^2 = 2m_1\partial_\omega m_1 \approx \partial_\omega(\omega^2/C_S^2 - n_1^2) = 2(\omega/C_S^2 - n_1\partial_\omega n_1). \tag{2.12}$$

For the last term, examine the vertical group velocity via

$$\begin{aligned}\partial_{n_1}\omega^2 &= 2\omega\partial_{n_1}\omega = \partial_{n_1}(-gn_1\tan n_1 h)\\ &= -g(\tan n_1 h + n_1 h\sec^2 n_1 h).\end{aligned} \tag{2.13}$$

Using the same approximation for small $(n_1h - \pi/2)$ as before then yields

$$\begin{aligned}\partial_{n_1}\omega &\approx \frac{g}{2\omega}\left[\frac{1}{n_1h-\pi/2} - \frac{n_1h}{(n_1h-\pi/2)^2}\right]\\ &= -\frac{\pi g}{4\omega}(n_1h-\pi/2)^{-2}.\end{aligned} \tag{2.14}$$

Inverting this and then using (2.8) yields the inverted vertical group velocity needed in (2.12):

$$\partial_\omega n_1 \approx -\left(\frac{4\omega}{\pi g}\right)(n_1h-\pi/2)^2 = -\frac{\pi g}{h^2\omega^3}. \tag{2.15}$$

Putting this into (2.12) then yields the inverse of the horizontal group velocity,

$$C_g^{-1} = \partial_\omega m_1 \approx \frac{\omega}{m_1}\left(\frac{1}{C_S^2} + \frac{n_1\pi g}{h^2\omega^4}\right) \approx \frac{\omega}{m_1}\left(\frac{1}{C_S^2} + \frac{\pi^2 g}{2h^3\omega^4}\right). \tag{2.16}$$

Ignoring the last term for now, the result is

$$C_g \approx C_S^2/C_P, \tag{2.17}$$

where $C_P \equiv \omega/m_1$ is the horizontal phase speed. It is clear from (2.10) that C_P is always larger than C_S, so the horizontal group velocity is always smaller (i.e., information cannot travel faster than the speed of sound). In fact, at the cutoff frequency, $m_1 = 0$ (by definition), and the horizontal group velocity is zero. At $\omega = 1\,\mathrm{rad\,s^{-1}}$ (6.28-s period), the horizontal group velocity is already up to $1212\,\mathrm{m\,s^{-1}}$ (with a phase velocity of $1856\,\mathrm{m\,s^{-1}}$); at $2\,\mathrm{rad\,s^{-1}}$, $C_g \approx 1433$ and $C_P \approx 1569\,\mathrm{m\,s^{-1}}$.

For the example values used above ($h = 4000\,\mathrm{m}$, $\omega \approx 0.6\,\mathrm{rad\,s^{-1}}$), the last term in the parentheses of (2.16) is about $(13\,\mathrm{km\,s^{-1}})^{-2}$, making it about 75 times smaller than the first term. As before, its importance decreases as frequency increases, or (because it also implies an increase in the cutoff frequency) as the water gets shallower. It therefore seems justifiable to neglect it in the ocean.

3. An alternative perspective

It stands out that in the above analysis for the "new modes" (imaginary n) the terms neglected include all those involving gravity, even those entering through the surface boundary condition (unlike for the "usual mode" or real n). It seems reasonable, then, to view these modes [which are not really new, having been identified over 100 years ago by Pidduck (1912)] as acoustic waves very slightly modified by the action of gravity, rather than as gravity waves dramatically modified by compressibility. Neglecting gravity, the equations are much simpler: to satisfy continuity [(1.9), dropping the negligible last term], try a potential of the form

$$\varphi = N\,\mathrm{Re}[e^{i(mx-\omega t)}(ae^{inz} + be^{-inz})], \tag{3.1}$$

representing waves progressing in x but allowing both upward and downward propagating components in z. The surface boundary condition neglecting gravity becomes (at $z = 0$)

$$\rho^{-1}p = -\partial_t\varphi = i\omega\varphi = 0, \tag{3.2}$$

which yields $b = -a$, so

$$\varphi = Na\,\mathrm{Re}[e^{i(mx-\omega t)}]\sin nz = Na\cos(mx-\omega t)\sin nz \tag{3.3}$$

(i.e., the waves are progressing in x but standing in z). Then the condition of no flow through the bottom becomes (at $z = -h$)

$$\partial_z\varphi = nNa\cos(mx-\omega t)\cos nh = 0. \tag{3.4}$$

So,

$$nh = \pi/2 + M\pi, \tag{3.5}$$

where M is any integer. These are simply the normal modes of the 4000-m thick oceanic waveguide with a rigid bottom and pressure-release surface (see, e.g., Jensen et al. 2011, chapter 2). As before, we associate n_1 with the smallest solution ($M = 0$); thus $n_1 = \pi/2h$, if this is physically allowed.

It should be noted here that according to the analysis of Jensen et al. (2011), for water over sediment and nonnormal incidence, the bottom boundary condition

(34) might more appropriately be approximated as a pressure-release condition [i.e., $\rho^{-1}p = -\partial_t\varphi = i\omega\varphi =$ const at $z = -h$, similar to (3.2)]. In that case, the gravest mode is a half-wavelength in the vertical rather than a quarter, and so the cutoff frequency is doubled, and every harmonic is a valid mode, not just the odd ones. This demonstrates that the actual underlying geology should be considered explicitly [as is indeed done in Cecioni et al. (2014) and Abdolali et al. (2015)]. For simplicity, the rigid bottom assumption is carried through here.

Now consider m_1 and n_1 for an acoustic wave traveling at an angle θ_1 off vertical:

$$m_1 = \frac{\omega}{C_S}\sin\theta_1 \quad \text{and} \quad n_1 = \frac{\omega}{C_S}\cos\theta_1 = \frac{\pi}{2h}. \tag{3.6}$$

The latter specifies

$$\theta_1 = \arccos\left(\frac{\pi C_S}{2h\omega}\right). \tag{3.7}$$

Thus, for θ_1 to be real requires $\omega \geq \pi C_S/2h$, just as in (2.11).

The horizontal group and phase speeds can also be reinterpreted:

$$C_P = \frac{\omega}{m_1} = \frac{C_S}{\sin\theta_1} \quad \text{and} \quad C_g = C_S\sin\theta_1 = \frac{C_S^2}{C_P}. \tag{3.8}$$

For $\omega = 1\ \mathrm{rad\,s^{-1}}$ and $h = 4000\ \mathrm{m}$, we find $\theta_1 = 54°$, and horizontal group speed is $C_g = 1212\ \mathrm{m\,s^{-1}}$ just as before. At $2\ \mathrm{rad\,s^{-1}}$, the angle is 73° off vertical (17° off horizontal), and C_g is $1433.5\ \mathrm{m\,s^{-1}}$, also as before. At $3\ \mathrm{rad\,s^{-1}}$, the angle is 78.7° (or 11.3° off horizontal), and C_g is $1471\ \mathrm{m\,s^{-1}}$.

In the case of excitation by some distant bottom motion, the highest frequencies, with C_g approaching C_S, should arrive first, with a distinctive sweep down toward the cutoff frequency. The first (highest frequency) arrivals may be confused, since they asymptotically cluster near C_S. Furthermore, since higher frequencies travel more nearly horizontally (for the same vertical mode), they are more susceptible to refraction in the sound channel and probably are not as strongly excited by the bottom motion. For waves more than 10° off horizontal, the above is probably robust; with the above values for h and C_S, this occurs at a frequency of about $3.4\ \mathrm{rad\,s^{-1}}$, for which the corresponding group velocity is about 98.5% of C_S.

Note that for the next vertical mode, $n_2 = 3\pi/2h = 3n_1$, and its cutoff frequency is also 3 times larger. Indeed, the second mode at $\omega = 3\ \mathrm{rad\,s^{-1}}$ would have the same angle off vertical as the mode-1 wave at $1\ \mathrm{rad\,s^{-1}}$ and hence the same horizontal group velocity. To generalize this, the frequency down-sweep would likely include a set of odd harmonics (due to all higher vertical modes) arriving at the same time as the mode-1 primary, up to a frequency where attenuation or rough bottom scattering damps them out (see Fig. 1).

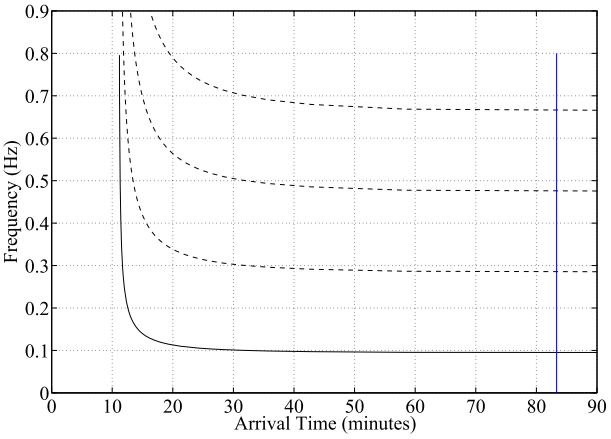

FIG. 1. Frequency vs arrival time for the first acoustic mode (solid) and three odd harmonics (dashed). The blue vertical line near 83 min denotes the arrival of the tsunami. The source in this example is 1000 km away in 4000-m-deep water, and the speed of sound is $1500\ \mathrm{m\,s^{-1}}$.

As a final note, for a point source on the bottom, it may be better to consider these waves as "rays" propagating up from the source, reflecting off the surface, and so on to the receiver, rather than vertical modes. This introduces the possibility that at a particular location some of the rays (and thus frequencies) might miss the receiver array. But surely many will hit and be heard.

4. Conclusions

As noted by Pidduck (1912), the full set of solutions to the equations such as laid out here fall into two distinct categories: one with real vertical wavenumber n that is strongly surface trapped and only slightly modified by compressibility (which he called "μ solutions"), and another class of modes with imaginary n that are oscillatory in depth (which he called "ν solutions"). In the course of making rational approximations to understand the predominant physics of acoustic–gravity surface waves, it came to light that the contribution of gravity acting on the "new modes" is quite small, comparable perhaps to the neglected effects of sound-speed variations or nonlinearity. It therefore seems advantageous to consider them as very slightly modified acoustic modes, which can be treated much more quickly, and for which other known effects can be included that may be more important in long-distance propagation (e.g., refraction,

nonlinearity, scattering, and subbottom propagation or penetration).

These results and interpretations do not conflict with earlier analyses: for example, while earlier work presents the maximum mode number at a given frequency, the analysis here is presented in the form of the minimum frequency at a given mode number. However, this acoustic perspective makes it easier to see that a set of odd harmonics (in frequency) should all arrive at the same time as the lowest ''new'' (or acoustic) mode.

This also does not detract from their possible use as an advance warning for tsunamis generated by deepwater bottom motion. Indeed, the identification of a discernable frequency down-sweep (including odd harmonics, see Fig. 1) may help distinguish arrivals from such a bottom-motion-induced ''point source'' versus distributed generation by other phenomena such as wave–wave interactions (cf. Kadri and Stiassnie 2013). In addition, the speed at which the frequency decreases is an indicator of the distance to the source and hence how long before any associated tsunami would arrive. In the example shown in Fig. 1 (source 1000 km away, other values as before), it appears feasible to identify this signature about 20 min after the generation, providing an hour warning before the tsunami strikes.

The earliest warning of a potential tsunami will most likely come from the global network of seismometers (e.g., Kurzon et al. 2014, and references therein). But these acoustic forerunners could be used in conjunction: the presence of an earthquake does not necessarily result in tsunamis, but the arrival of the acoustic signature of bottom motion would indicate a much greater probability. In addition, the seismic information would indicate just when (and from what direction) to look for such a signature. Indeed, work toward implementing this in real time is well under way (see, e.g., Cecioni et al. 2014; Abdolali et al. 2015).

Finally, it should be reiterated that the bottom boundary condition in the real ocean is neither rigid nor pressure release; the actual geology and acoustic propagation below the bottom needs to be considered, as is indeed done in Cecioni et al. (2014) and Abdolali et al. (2015).

Acknowledgments. This work was supported by the University of California, San Diego. I would also like to thank an anonymous reviewer and R. Salmon and the students and postdocs in the ''wave-mean-flow club'' at Scripps Institution of Oceanography for finding errors and helping smooth out kinks in the presentation.

REFERENCES

Abdolali, A., C. Cecioni, G. Bellotti, and J. T. Kirby, 2015: Hydro-acoustic and tsunami waves generated by the 2012 Haida Gwaii earthquake: Modeling and in situ measurements. *J. Geophys. Res. Oceans*, **120**, 958–971, doi:10.1002/2014JC010385.

Cecioni, C., G. Bellotti, A. Romano, A. Abdolali, P. Sammarco, and L. Franco, 2014: Tsunami early warning system based on real-time measurements of hydro-acoustic waves. *Proc. Eng.*, **70**, 311–320, doi:10.1016/j.proeng.2014.02.035.

——, A. Abdolali, G. Bellotti, and P. Sammarco, 2015: Large-scale numerical modeling of hydro-acoustic waves generated by tsunamigenic earthquakes. *Nat. Hazards Earth Syst. Sci.*, **15**, 627–636, doi:10.5194/nhess-15-627-2015.

Hendin, G., and M. Stiassnie, 2013: Tsunami and acoustic-gravity waves in water of constant depth. *Phys. Fluids*, **25**, 086103, doi:10.1063/1.4817996.

Jensen, F. B., W. A. Kuperman, M. B. Porter, and H. Schmidt, 2011: *Computational Ocean Acoustics*. 2nd ed. Springer, 794 pp.

Kadri, U., 2014: Deep ocean water transport by acoustic-gravity waves. *J. Geophys. Res.*, **119**, 7925–7930, doi:10.1002/2014JC010234.

——, 2015: Wave motion in a heavy compressible fluid: Revisited. *Eur. J. Mech. B: Fluids*, **49A**, 50–57, doi:10.1016/j.euromechflu.2014.07.008.

——, and M. Stiassnie, 2012: Acoustic-gravity waves interacting with the shelf break. *J. Geophys. Res.*, **117**, C03035, doi:10.1029/2011JC007674.

——, and ——, 2013: Generation of an acoustic-gravity wave by two gravity waves, and their subsequent mutual interaction. *J. Fluid Mech.*, **735**, R6, doi:10.1017/jfm.2013.539.

Kurzon, I., F. L. Vernon, A. Rosenberger, and Y. Ben-Zion, 2014: Real-time automatic detectors of P and S waves using singular value decomposition. *Bull. Seismol. Soc. Amer.*, **104**, 1696–1708, doi:10.1785/0120130295.

Lamb, H., 1932: *Hydrodynamics.* 6th ed. Dover, 738 pp.

Pidduck, F. B., 1912: The wave-problem of Cauchy and Poisson for finite depth and slightly compressible fluid. *Proc. Roy. Soc. London*, **86**, 396–405, doi:10.1098/rspa.1912.0031.

Stiassnie, M., 2010: Tsunamis and acoustic-gravity waves from underwater earthquakes. *J. Eng. Math.*, **67**, 23–32, doi:10.1007/s10665-009-9323-x.

Tolstoy, I., and C. S. Clay, 1987: *Ocean Acoustics: Theory and Experiment in Underwater Sound.* Acoustical Society of America, 381 pp.

Watada, S., 2013: Tsunami speed variations in density-stratified compressible global oceans. *Geophys. Res. Lett.*, **40**, 4001–4006, doi:10.1002/grl.50785.